

Synthesis and Characterization of Diamond Microcrystals and Nanorods Deposited by Hot Cathode Direct Current Plasma Chemical Vapor Deposition Method

Leyong Zeng,^{†,‡} Hongyan Peng,[§] Weibiao Wang,^{*,†} Yuqiang Chen,[§] Da Lei,^{†,‡} Wentao Qi,[§] Jingqiu Liang,^{||} Jialong Zhao,[†] Xianggui Kong,[†] and Hong Zhang[⊥]

Key Laboratory of Excited State Processes, Changchun Institute of Optics, Fine Mechanics and Physics, Chinese Academy of Sciences, Changchun, 130033, People's Republic of China, Graduate School of Chinese Academy of Sciences, Beijing, 100049, People's Republic of China, Department of Physics, Mudanjiang Normal College, Mudanjiang, 157012, People's Republic of China, State Key Laboratory of Applied Optics, Changchun Institute of Optics, Fine Mechanics and Physics, Chinese Academy of Sciences, Changchun 130033, People's Republic of China, and Van't Hoff Institute for Molecular Sciences, University of Amsterdam, Nieuwe Achtergracht 166, 1018 WV Amsterdam, The Netherlands

Received: November 19, 2007; In Final Form: February 5, 2008

(111) diamond microcrystals and (100) diamond microcrystals and nanorods were synthesized on Si substrate by hot cathode direct current plasma chemical vapor deposition method. The morphology, structure, and optical properties of the diamond films were characterized by scanning electron microscopy, X-ray diffraction, Raman spectra, and Fourier transform infrared spectra. The results showed that (111) and (100) diamond films can be grown under the condition of high-temperature (1223 K), low CH₄ concentration (4/300 sccm) and low temperature (1098 K), high CH₄ concentration (6/300 sccm), respectively. The (100) diamond film has lower purity and quality but higher optical transmittance than the (111) diamond film. Thus, the reactor temperature and CH₄ concentration are responsible for the growth of diamond films.

1. Introduction

Diamonds have many exceptional properties, such as extreme hardness, high thermal conductivity, high optical transmittance, wide band gap, low electron work function, high chemical stability, and so on.^{1,2} Therefore, diamond films have potential applications in many fields such as hard surface coatings, flat panel displays, detectors and sensors, optical windows, surface acoustic wave (SAW) devices, electrochemical electrodes, and so forth.^{3–11} In previous reports, diamond films have typically been synthesized by hot filament, direct current plasma, and microwave plasma chemical vapor deposition methods, and the used gas is mainly CH₄/H₂ gas mixture for microcrystalline diamonds and CH₄/H₂ or CH₄/Ar/H₂ gas mixture for nanocrystalline diamonds.^{12–15} Furthermore, diamond nanowires and nanorods have been prepared by microprocess technology, etching of diamond films or carbon nanotubes.^{16–19} It is generally agreed that the properties of diamond films, such as morphology, microstructure, and quality, determine the suitability for the particular applications.^{20,21} For example, high-quality diamond films can be used for mechanical coatings and thermal conductivity materials because of their high hardness and exceptional thermal conductivity. (100) diamond films can be good optical window materials because of the high transmittance of (100) plane diamond films. Specifically, diamond nanorod arrays can be used as electron emitters for field emission displays, and single diamond nanorods can be used

as probes for the atom force microscope, scanning tunnel microscope, and other reamers. However, in past reports, one-dimensional diamond nanomaterials, for example, diamond nanorods, nanowires, and nanowimble, were mainly prepared by microprocess technology. In the process, the diamond films were first deposited, and then nanowimble or nanorods were formed by the etching of films. The difficulty of the microprocess technology is high, and the cost is also expensive, which are unfavorable for the applications. Therefore, for the synthesis of diamond films with different morphologies, the experimental parameters must be carefully controlled to obtain high-quality diamond films. In our previous work, nanocrystalline diamond films with different grain sizes, surface smoothness and quality have been prepared on Si substrate by changing the composition of CH₄/Ar/H₂ gas mixture using hot cathode direct current chemical vapor deposition (DC–PCVD) method.²² Hot cathode DC–PCVD method is an effective method for the deposition of diamond films (including nanocrystalline, microcrystalline diamond films, etc.), and diamond films can be deposited uniformly with large area and high growth rate. Therefore, the study of hot cathode DC–PCVD synthesis is interesting for the applications of diamond based devices.

In this paper, we report the synthesis of (111) diamond microcrystals and (100) diamond microcrystals and nanorods on Si substrate by hot cathode DC–PCVD method, using a CH₄/H₂ gas mixture. We study the morphology, structure, and optical properties of diamond films by scanning electron microscopy (SEM), X-ray diffraction (XRD), Raman spectroscopy, and Fourier transform infrared (FT-IR) spectroscopy. Finally, we discuss the effect of reactor temperature and CH₄ concentration on the growth of diamond films.

* Corresponding author. E-mail: wangwb@126.com.

[†] Key Laboratory of Excited State Processes, Changchun Institute of Optics, Fine Mechanics and Physics, Chinese Academy of Sciences.

[‡] Graduate School of Chinese Academy of Sciences.

[§] Mudanjiang Normal College.

^{||} State Key Laboratory of Applied Optics, Changchun Institute of Optics, Fine Mechanics and Physics, Chinese Academy of Sciences.

[⊥] University of Amsterdam.

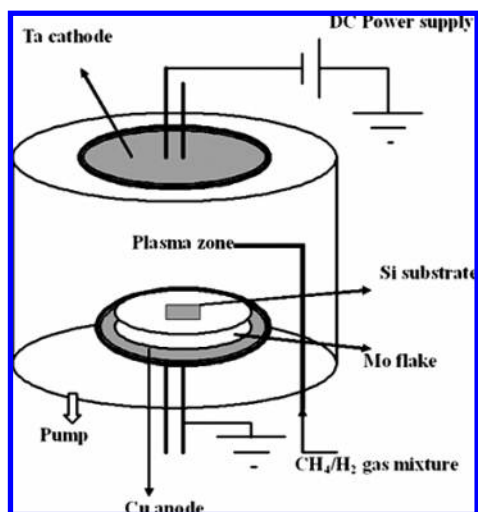


Figure 1. Schematic diagram of hot cathode DC-PCVD system for the deposition of diamond films.

TABLE 1: Experimental Parameters for the Growth of (111) Diamond and (100) Diamond Films

samples	CH ₄ :H ₂ (sccm)	T (K)	chamber pressure (Pa)	DC voltage (V)	DC current (A)	deposition time (h)
(111) diamond	4:300	1223	1.5×10^4	800	6.5	5
(100) diamond	6:300	1098	1.25×10^4	690	6	5

2. Experimental Section

Diamond films were prepared on Si (100) substrate by hot cathode DC-PCVD method. Before the experiment, the Si wafers were ultrasonically scratched in ethanol with 500 nm diamond powder for about 10 min, and then were ultrasonically cleaned in deionized water for 10 min. The schematic diagram of hot cathode DC-PCVD system was shown in Figure 1. The spacing between Ta cathode and Cu anode was about 5 cm, and the Ta cathode was linked with high voltage DC power supply. The Si wafer was placed onto a Mo flake to contact with the Cu anode. Before the deposition of diamond films, the chamber pressure was pumped out to below 6×10^{-2} Pa, and then H₂ gas with a flow rate of 300 sccm was introduced into the chamber to produce glow discharge along with the increase of DC voltage. When the glow discharge was stable, CH₄ gas was introduced into the chamber. The substrate temperature was adjusted by DC voltage and chamber pressure and was measured by an infrared temperature sensor. Then the diamond microcrystals and nanorods were deposited on Si substrate with different experimental conditions, respectively. The experimental parameters for the growth of diamond films with different morphologies were shown in Table 1. The flow ratio of CH₄/H₂ and deposition time are 4/300, 5 h and 6/300, 5 h for the growth of (111) and (100) diamond films, respectively. Finally, the gas valves and power supply were shut off, and the chamber pressure was pumped out to below 6×10^{-2} Pa.

The morphology, microstructure, and optical properties of diamond microcrystals and nanorods were characterized by scanning electron microscope (Hitachi S-4800) operated with an accelerating voltage of 20 kV, X-ray diffractometer (Rigaku D/MAX 2200VPC) with Cu K α radiation, Raman spectrometer (Renishaw inVia) at the laser wavelength of 514.5 nm from an Ar⁺ laser, and Fourier transform infrared spectrometer (IRPrestige-21).

3. Results and Discussion

Figure 2 shows the low-resolution SEM images of diamond films with different morphologies. As seen in Figure 2a, the diamond microcrystals have triangle structures, which indicates the (111) orientation of microcrystalline diamonds, and the sizes of single diamond microcrystal range from about 5 to 15 μ m. Moreover, the surface smoothness of the (111) diamond film is also not well. In Figure 2b, the diamond film consists of microcrystals and nanorods. The diamond microcrystals have quadrangle structures, which indicates the (100) orientation of diamond film, and the sizes of single diamond microcrystals range from 3 to 12 μ m. Some surfaces of every diamond microcrystal are smooth, but some diamond nanorods are grown on the other surface of the diamond microcrystal.

Figure 3 shows the high-resolution SEM images of diamond films with different morphologies. As shown in Figure 3a, the (111) facet of diamond can be clearly observed. The opposite two facets are smooth and have scalariform structure, but the other two facets are rough and consist of diamond nanocrystals. In Figure 3b, it can be noted that the width of steps is about 200 nm, and the size of diamond nanocrystals is about 100 nm. As seen in Figure 3c, the (100) diamond microcrystals and nanorods are distributed disorderly on the substrate. The surfaces of single diamond microcrystals have stripe structure but are still smooth. The diamond nanorods are grown vertically on the other surface of diamond microcrystals. In Figure 3d, it can be observed that the thickness of diamond microcrystals is about 1.10 μ m, and the diameter of diamond nanorods is about 50 nm. It can also be noted that the surface of diamond microcrystals on which diamond nanorods are grown is not smooth but consists of diamond nanocrystals with the sizes of about 100 nm.

The XRD patterns of (111) diamond microcrystals and (100) diamond microcrystals and nanorods are shown in Figure 4. It can be seen that the synthesized diamond films are polycrystalline diamond films. In the XRD pattern of (111) diamond microcrystals, the peaks of (111), (220), and (311) of diamonds with cubic structure can be observed at $2\theta = 43.9^\circ$, 75.3° , and 91.5° , respectively, and the intensity of (111) peak is largest in all. However, the peaks of diamond (400) and Si (400) are increased in the XRD pattern of (100) diamond microcrystals and nanocrystals at $2\theta = 119.5^\circ$ and 69.1° , respectively. The broad peak of Si (400) comes from the substrate, which can be attributed to the small thickness or the bad uniformity of diamond films because of the structural presence of microcrystals and nanorods. The peak of diamond (400) indicates the presence of (100) facet of diamond. The results indicate that (100) diamond film has lower density and thickness than (111) diamond film because of the presence of diamond nanorods but has the same good crystal quality as (111) diamond film.

Figure 5 shows the Raman spectra of (111) diamond microcrystals and (100) diamond microcrystals and nanorods. In general, the strong peak at about 1332 cm^{-1} and the broad peak at about 1500–1600 cm^{-1} can be observed in the Raman spectrum of microcrystalline diamond. The peak at about 1332 cm^{-1} corresponds to the characteristic peak of diamond. The broad peak at about 1500–1600 cm^{-1} is related to the presence of disordered sp³ structure or non-diamond phase in diamond films. Furthermore, the intensity ratio of diamond peak to non-diamond peak implies the purity and quality of diamond films. As seen in Figure 5, only the characteristic peak of diamond at about 1332 cm^{-1} appears in the Raman spectrum of (111) microcrystalline diamond films. However, other than the strong peak at about 1332 cm^{-1} , the broad weak peak at about

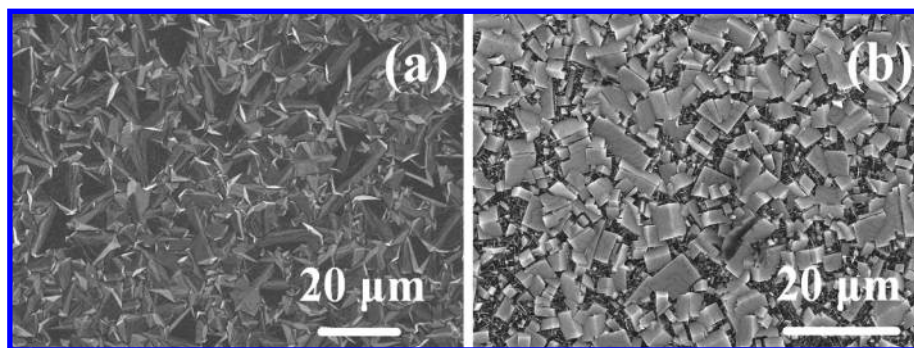


Figure 2. Low-resolution SEM images of (111) diamond microcrystals (a) and (100) diamond microcrystals and nanorods (b).

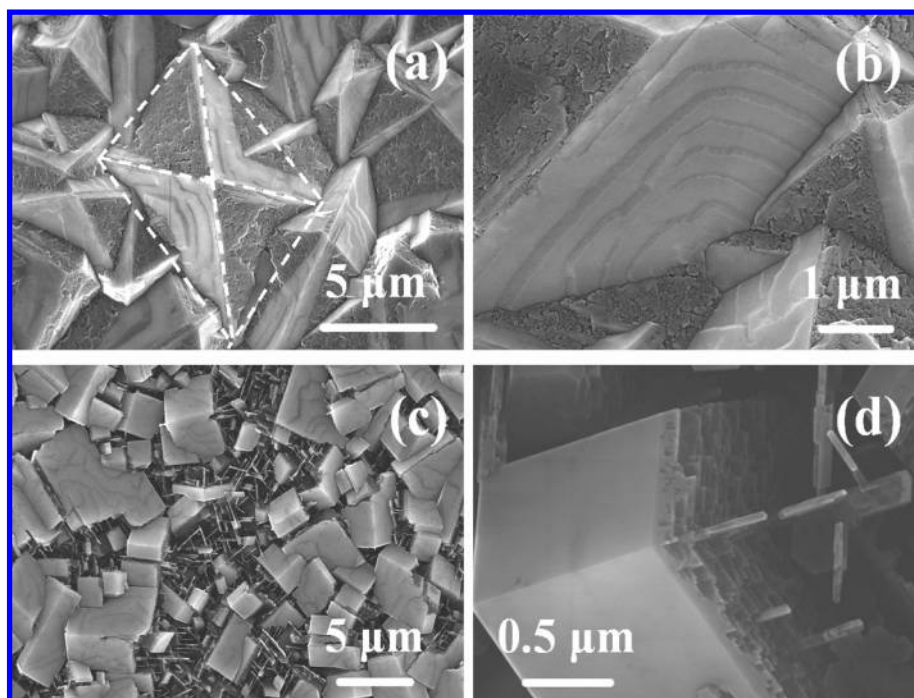


Figure 3. High-resolution SEM images of (111) diamond microcrystals (a,b) and (100) diamond microcrystals and nanorods (c,d).

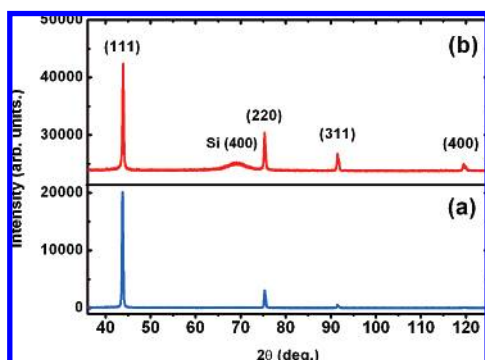


Figure 4. XRD patterns of (111) diamond microcrystals (a) and (100) diamond microcrystals and nanorods (b).

$1500\sim 1600\text{ cm}^{-1}$ can also be observed in the Raman spectrum of (100) diamond microcrystals and nanorods. It is well-known that the value of full width at half-maximum (fwhm) of diamond peak exhibits the disorder degree and defects quantity in diamond films, and the increase of fwhm value can be correlated with the decrease of grain sizes.^{23–25} As shown in Figure 5, the fwhm values of (111) and (100) diamond films can be estimated to be about 8.2 and 11 cm^{-1} , respectively. This indicates that the quality of (111) diamond film was better than that of (100) diamond film, but the grain sizes of (100) diamond is smaller

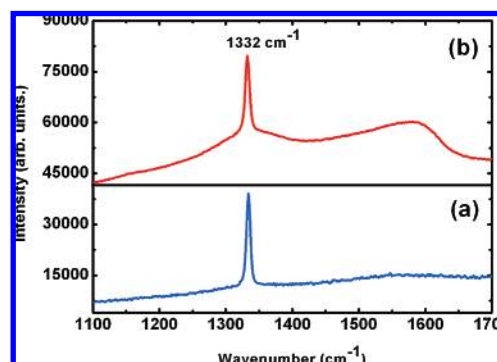


Figure 5. Raman spectra of (111) diamond microcrystals (a) and (100) diamond microcrystals and nanorods (b).

than that of (111) diamond, which is also in accordance with the results of SEM. In comparison with the Raman spectra of (111) and (100) diamond films, it can be concluded that the (111) microcrystalline diamond film has higher purity and quality than the (100) diamond microcrystals and nanorods.

Figure 6 shows the FT-IR transmission spectra of (111) diamond microcrystals and (100) diamond microcrystals and nanorods, recorded in the wavenumber range of $400\text{--}3500\text{ cm}^{-1}$. The broad absorption band between 1333 and 2666 cm^{-1} corresponds to the two-phonon absorption, which is intrinsic

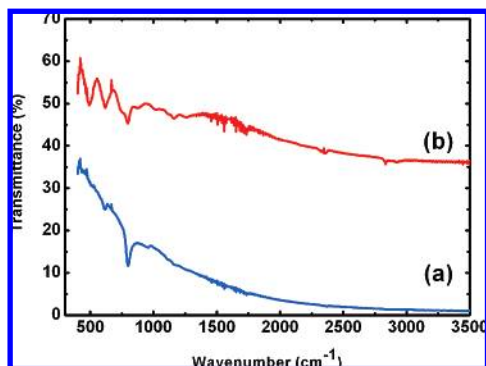


Figure 6. FT-IR spectra of (111) diamond microcrystals (a) and (100) diamond microcrystals and nanorods (b).

for pure diamond.^{26,27} The series of absorption bands below 1333 cm^{-1} are related to one-phonon absorption of impurities and defects in diamond films.²⁷ It is obviously observed that one-phonon absorption becomes stronger in the (100) diamond film than that in the (111) diamond film, which indicates that (111) diamond film has lower impurities and defects than (100) diamond film. In the FT-IR spectrum of (100) diamond film, the small absorption band at about 2830 cm^{-1} is associated with the C–H stretching vibration mode of diamond films.^{27–29} And the band at about 797 cm^{-1} originates from the transverse optical phonon mode of Si–C bonds formed during the original growth stage of diamond films.^{29–31} It can also be seen that (100) diamond film has higher transmittance than (111) diamond film. The high transmittance of (100) diamond film is related to the properties of (100) facet and the smooth surface. This indicates that (100) diamond film is more suitable for its application in optical windows.

On the basis of the above results, it can be found that the reactor temperature and CH_4 concentration have an important effect on the morphology, structure, purity, and optical properties of diamond films. Therefore, it can be concluded that the high-temperature (1223 K) is favorable for the growth of (111) microcrystalline diamond films with high purity and high quality. Diamond nanocrystals can be grown oriented (111) facet to constitute (111) diamond microcrystals, and the nucleation is accordant with the model of step growth. However, the low temperature (1098 K) can lead to the growth of (100) microcrystalline diamonds and even decrease the grain sizes to form diamond nanorods. Moreover, the low temperature can also decrease the quality of diamond films and is favorable for the deposition of disordered sp^3 or sp^2 bonded carbon. Diamond nanocrystals can be grown oriented (100) facet to constitute (100) diamond microcrystals. In comparison with CH_4 concentration in the two experiments, it can also be concluded that high CH_4 concentration can decrease the grain sizes of diamond films, but can also increase the impurities and defects in diamond films. Therefore, the high temperature, low CH_4 concentration and low temperature, high CH_4 concentration are responsible for the synthesis of (111) and (100) diamond films, respectively.

Diamond films with different morphologies may have potential applications in many fields. The (111) high-purity diamond films can be applied in micromechanical systems sensors, SAW filters, and so forth. Moreover, boron-doped (111) diamond films can be a good candidate for electrode materials to be used in the electrochemical field. Because of the high transmittance, (100) diamond films can be used as windows materials in the applications of large-power infrared lasers, detectors, and so on. Furthermore, the diamond nanorods grown on microcrystalline diamond films will probably be used as

cutting tools and cold cathode emitters. Furthermore, the hot cathode DC–PCVD method has an advantage for fabricating diamond films, compared with other methods. First, by using this method, diamond films can be fabricated with large area; moreover, the films are uniform in different parts. Second, by using this method, diamond films can be fabricated with high growth rates, and the nucleation of diamond is easier. Third, using this method, we can accurately control the morphology and structure of diamond films. Therefore, the hot cathode DC–PCVD synthesis and characterization of diamond films will be interesting for broadening the potential applications of diamond microcrystals and nanorods in many fields.

4. Conclusion

In summary, diamond microcrystals and nanorods were synthesized on Si substrate by hot cathode DC–PCVD method. The high-temperature (1223 K) and low CH_4 concentration led to the growth of (111) microcrystalline diamond films, but the low temperature (1098 K) and high CH_4 concentration can lead to the growth of (100) diamond microcrystals and nanorods. Furthermore, the low reactor temperature and high CH_4 concentration decreased the grain sizes, purity, and quality of diamond films but increased the transmittance of diamond films. The (111) and (100) diamond films may have potential applications in electrochemical hardness tools, optoelectronics fields, and so on.

Acknowledgment. This work was supported by the National Natural Science Foundation of China (NSFC, Grants 50072029 and 50572101) and tackle hard-nut program in science and technology of Heilongjiang Province of China (Grant 2006G2016-00). Furthermore, the authors would also like to thank Dr. Zhu Ruihua for help with the SEM test.

References and Notes

- (1) Angus, J. C.; Hayman, C. C. *Science* **1998**, *241*, 913.
- (2) Yarbrough, W. A.; Messier, R. *Science* **1990**, *247*, 688.
- (3) Lu, X.; Yang, Q.; Chen, W.; Xiao, C.; Hirose, A. *J. Vac. Sci. Technol.* **2006**, *24*, 2575.
- (4) Ternyak, O.; Akhvediani, R.; Hoffman, A.; Wong, W. K.; Lee, S. T.; Lifshitz, Y.; Daren, S.; Cheifetz, E. *J. Appl. Phys.* **2005**, *98*, 123522.
- (5) Yu, J. J.; Boyd, I. W. *Diam. Relat. Mater.* **2007**, *16*, 494.
- (6) Nebel, C.; Rezek, B.; Shin, D.; Uetsuka, H.; Yang, N. *J. Phys. D* **2007**, *40*, 6443.
- (7) Wang, S. F.; Hsu, Y. F.; Pu, J. C.; Sung, J. C.; Hwa, L. G. *Mater. Chem. Phys.* **2004**, *85*, 432.
- (8) Stolarczyk, K.; Nazaruk, E.; Rogalski, J.; Bilewicz, R. *Electrochem. Commun.* **2007**, *9*, 115.
- (9) Ferro, S.; Battisti, A. D. *J. Phys. Chem. B* **2003**, *107*, 7567.
- (10) Singh, R. K.; Gilbert, D. R.; Laveigne, J. *Appl. Phys. Lett.* **1996**, *69*, 2181.
- (11) Wu, D.; Ma, Y. C.; Wang, Z. L.; Luo, Q.; Gu, C. Z.; Wang, N. L.; Li, Lu, C. Y.; X. Y.; Jin, Z. S. *Phys. Rev. B* **2006**, *73*, 012501.
- (12) Sharda, T.; Rahaman, M. M.; Nukaya, Y.; Soga, T.; Jimbo, T.; Umeno, M. *Diam. Relat. Mater.* **2001**, *10*, 561.
- (13) Suzuki, T.; Ishihara, T.; Shimosato, T.; Yamazaki, T.; Wada, S. J. *Eur. Ceram. Soc.* **1998**, *18*, 141.
- (14) Michaelson, S.; Lifshitz, Y.; Ternyak, O.; Akhvediani, R.; Hoffman, A. *Diam. Relat. Mater.* **2007**, *16*, 845.
- (15) Huang, S. M.; Hsu, H. C.; You, M. S.; Hong, F. C. N. *Diam. Relat. Mater.* **2006**, *15*, 22.
- (16) Baik, E. S.; Baik, Y. J.; Jeon, D. J. *Mater. Res.* **2000**, *15*, 923.
- (17) Ando, Y.; Nishibayashi, Y.; Sawabe, A. *Diam. Relat. Mater.* **2004**, *13*, 633.
- (18) Sun, L. T.; Gong, J. L.; Zhu, Z. Y.; Zhu, D. Z.; Wang, Z. X.; Zhang, W.; Hu, J. G.; Li, Q. T. *Diam. Relat. Mater.* **2005**, *14*, 749.
- (19) Sun, L. T.; Gong, J. L.; Zhu, Z. Y.; He, S. X. *Adv. Mater.* **2004**, *16*, 1849.
- (20) Muller, S. W.; Worner, E.; Fuchs, F.; Wild, C.; Koidl, P. *Appl. Phys. Lett.* **1996**, *68*, 759.
- (21) Ahmed, W.; Rego, C. A.; Cherry, R.; Afzal, A.; Ali, N.; Hassan, I. U. *Vacuum* **2000**, *56*, 153.

- (22) Zeng, L. Y.; Peng, H. Y.; Wang, W. B.; Chen, Y. Q.; Lei, D.; Qi, W.; Liang, J. Q.; Zhao, J. L.; Kong, X. G.; Zhang, H. *J. Phys. Chem. C* **2008**, *112*, 1401.
- (23) Nemanich, R. J.; Glass, J. T.; Lucovsky, G.; Shroder, R. E. *J. Vac. Sci. Technol.* **1988**, *6*, 1783.
- (24) Shroder, R. E.; Nemanich, R. J.; Glass, J. T. *Phys. Rev. B* **1990**, *41*, 3738.
- (25) Piazza, F.; Gonzalez, J. A.; Velazquez, R.; De Jesus, J.; Rosario, S. A.; Morell, G. *Diam. Relat. Mater.* **2006**, *15*, 109.
- (26) Vogelgesang, R.; Alvarenga, A. D.; Hyun Jung, K.; Ramdas, A. K.; Rodriguez, S.; Grimsditch, M.; Anthony, T. R. *Phys. Rev. B* **1998**, *58*, 5408.
- (27) McNamara, K. M.; Williams, B. E.; Gleason, K. K.; Scruggs, B. E. *J. Appl. Phys.* **1994**, *76*, 2466.
- (28) Dischler, B.; Wild, C.; Muller-Sebert, W.; Koidl, P. *Phys. B* **1993**, *185*, 217.
- (29) Tang, C. J.; Neves, A. J.; Fernandes, A. J. S. *Diam. Relat. Mater.* **2003**, *12*, 1488.
- (30) Tang, C. J.; Neves, A. J.; Fernandes, A. J. S. *Diam. Relat. Mater.* **2003**, *12*, 251.
- (31) Woo, H. K.; Lee, C. S.; Bello, I.; Lee, S. T. *J. Appl. Phys.* **1998**, *83*, 4187.